Bioenerg. Res. (2010) 3:272–277
DOI 10.1007/s12155-010-9079-1

Imaging Lignin-Downregulated Alfalfa Using Coherent Anti-Stokes Raman Scattering Microscopy

Yining Zeng · Brian G. Saar · Marcel G. Friedrich · Fang Chen · Yu-San Liu · Richard A. Dixon · Michael E. Himmel · X. Sunney Xie · Shi-You Ding

Published online: 25 February 2010

Abstract Targeted lignin modification in bioenergy crops could potentially improve conversion efficiency of lignocellulosic biomass to biofuels. To better assess the impact of lignin modification on overall cell wall structure, wild-type and lignin-downregulated alfalfa lines were imaged using coherent anti-Stokes Raman scattering (CARS) microscopy. The 1,600-cm^{-1} Raman mode was used in CARS imaging to specifically represent the lignin signal in the plant cell walls. The intensities of the CARS signal follow the general trend of lignin contents in cell walls from both wild-type and lignin-downregulated plants. In the downregulated lines, the overall reduction of lignin content agreed with the previously reported chemical composition. However, greater reduction of lignin content in cell corners was observed by CARS imaging, which could account for the enhanced susceptibility to chemical and enzymatic hydrolysis observed previously.

Keywords Lignin · Chemical image · Coherent anti-Stokes Raman scattering (CARS) · Lignin-downregulated alfalfa

Y. Zeng · Y.-S. Liu · M. E. Himmel · S.-Y. Ding (✉)
Biosciences Center,
National Renewable Energy Laboratory,
1617 Cole Boulevard,
Golden, CO 80401, USA
email: Shi.you.Ding@nrel.gov

B. G. Saar · M. G. Friedrich · X. S. Xie (✉)
Department of Chemistry and Chemical Biology,
Harvard University,
12 Oxford Street,
Cambridge, MA 02138, USA
email: xie@chemistry.harvard.edu

F. Chen · R. A. Dixon
Plant Biology Division, Samuel Roberts Noble Foundation,
2510 Sam Noble Parkway,
Ardmore, OK 73401, USA

Y. Zeng · F. Chen · Y.-S. Liu · R. A. Dixon · M. E. Himmel · S.-Y. Ding
Bioenergy Science Center (BESC),
Oak Ridge National Laboratory,
Oak Ridge, TN, USA

Introduction

Lignocellulosic biomass is under consideration as a sustainable and renewable source for fuels and chemicals [1]. One of the major technical barriers to commercialization of this technology is the high cost of the chemical/biological processes that deconstruct the insoluble polymeric plant cell wall materials into soluble sugars [2]. To improve the above processes, deeper understanding of the chemical and structural architectures of plant cell walls is required and new imaging tools are essential to achieve this goal. Over the past few years, nonlinear optical microscopy, such as coherent anti-Stokes Raman scattering (CARS), has been demonstrated to be a powerful tool for chemical imaging of biological systems [3]. CARS microscopy provides a contrast mechanism based on molecular vibrations, which are intrinsic to the samples, as well as high spatiotemporal resolution, and is free of background from one-photon-excited fluorescence [4]. Two laser beams, pump (at frequency ω_p) and Stokes (at frequency ω_s), are temporally and spatially overlapped to generate anti-Stokes signals at frequency $\omega_{as} = 2\omega_p - \omega_s$ such that the frequency difference ($\omega_p - \omega_s$) is tuned to match a particular Raman-active vibration frequency. The resonant CARS signal is orders of magnitude greater than that from spontaneous Raman scattering. CARS offers much greater sensitivity and faster acquisition time than traditional Raman and has been widely used to characterize complex materials [5].

Higher plant cell walls are composed of lignin and various polysaccharides which are blended into a complex three-dimensional matrix [6]. In plant anatomy, lignin provides the necessary mechanical support for stem strength and general cell integrity and acts as a water barrier in lignified tissues [7, 8]. In biomass conversion, lignin contributes to biomass recalcitrance by blocking access of enzymes to cell wall polysaccharides, therefore limiting saccharification efficiency [9]. Removal of lignin therefore constitutes an important obstacle for efficient biomass conversion. Although it is still not clear how lignin content and composition affect the chemical/enzymatic hydrolysis of feedstocks in general, it has been demonstrated that the pulping of trees and digestibility of forages can be improved by downregulating genes encoding enzymes of monolignol biosynthesis [10]. Recently, Chen et al. [11] demonstrated that lignin modification indeed improves sugar yields during the saccharification processes for bioethanol production. In their study, the lignin biosynthesis pathway was downregulated independently at six different enzymatic steps in alfalfa (*Medicago sativa* L.). It was shown that the lignin content was negatively correlated to the levels of sugars released by enzymatic hydrolysis. It is also important to determine how the lignin distribution in the cell wall is affected by the downregulation of lignin biosynthesis. To this end, in the present work, wild-type (WT) and two previously generated transgenic alfalfa lines, in which hydroxycinnamoyl CoA: shikimate hydroxycinnamoyl transferase (HCT) or coumaroyl shikimate 3-hydroxylase (C3H) are downregulated [12], were imaged by CARS microscopy.

Methods

Alfalfa Sample Preparation

The WT and transgenic alfalfa lines downregulated in HCT and C3H were grown and harvested in the greenhouse. Details of the HCT and C3H lines and growth condition were reported previously [11]. For this study, ~20 slices of the sixth internodes of one independent line of WT, HCT, and C3H were analyzed. Fresh alfalfa stem samples were harvested and stored at −80°C. The sample was hand-cut into slices 25–50 μm thick by using a single-blade razor. These cross-sections were kept in distilled water prior to CARS measurement. For CARS measurement, the stem slices were kept in distilled water between two glass coverslips.

CARS Imaging

The CARS images were acquired on a Zeiss LSM5-MP/DuoScan NIR CARS microscope. A mode-locked Nd:YVO_4 laser (High Q Laser (US), Inc.) was used to generate a 7-ps, 76-MHz pulse train of both 1,064-nm (1-W average power) and 532-nm (5-W average power) laser beams. The 1,064-nm beam was used as the CARS Stokes beam. The 532-nm beam was used to pump an optical parametric oscillator (Levante Emerald, APE-Berlin) in order to generate the CARS pump beam, which was a 6-ps pulse train at 910 nm (1-W average power). The pump and Stokes pulse trains were overlapped in time using a delay stage and sent collinearly into the microscope. The two beams were focused onto the sample through a Zeiss C-Apochromat 40×1.1 UV–VIS-IR water immersion objective. This setup gives lateral resolution of ~350 nm. The excitation power after the objective was kept at ~200 mW for the pump and ~100 mW for the Stokes beam.

CARS images were obtained by raster scanning the collinear pump and Stokes pulses over the sample and collecting the anti-Stokes light. The anti-Stokes light was collected both in the Epi direction via the objective lens and the forward direction via the microscope air condenser. The anti-Stokes light was separated from the pump and the Stokes beams by a bandpass filter (HQ750/210, Chroma Technology) in the forward CARS direction and by a long-wave pass dichroic mirror (880DXXR, Chroma Technology) in combination with a bandpass filter (HQ750/210, Chroma Technology) for the Epi-CARS channel. The residual two-photon-excited fluorescence signal in the Epi direction was removed by a narrowband cleanup filter (HQ800/40 m, Chroma Technology).

To obtain autofluorescence micrographs of the entire stem, a slice of the stem was prepared by microtome and imaged on an Olympus IX71 microscope using an Olympus 4×/0.13 PhL objective lens. The image was captured by an Olympus DP70 camera.

Results and Discussion

Cell wall lignins consist primarily of phenylpropane units [13] that show a characteristic Raman vibrational mode at 1,600 cm^{-1} due to the symmetric aromatic ring C=C stretch [14, 15]. Therefore, the CARS signal was carefully adjusted to match this vibrational mode to provide chemically specific imaging of lignin. Phenylalanine and tyrosine residues in cell wall proteins may also have similar symmetric phenol ring structures. However, due to the significantly lower amount of such molecules in cell walls compared to lignin, the CARS signal at 1,600 cm^{-1} contributed by proteins is negligible. Indeed, in some protein-rich tissues, for example phloem, no significant CARS signal was observed.

The CARS microscope was configured to detect signals from both forward CARS (F-CARS) and backward (Epi-CARS) directions simultaneously. The specificity of

the CARS signal was proven by alternately blocking the pump beam and the Stokes beam. Figure 1 shows the scanning images of F-CARS and Epi-CARS, the multi-photon fluorescence (MPF) generated by the 910-nm pump beam, and the MPF generated by the 1,064-nm Stokes beam. The strong CARS signal disappeared when either the pump or the Stokes beam was blocked (Fig. 1c, d). When the two laser pulses were temporally offset or blocked, the signal also vanished, which rules out any significant contributions from multi-photon fluorescence. To further confirm the specificity of the CARS signal, the CARS frequency was tuned slightly away from 1,600 cm^{-1}. The strong signal decreases significantly, which proves that a substantial part of the signal was indeed due to CARS from lignin (Fig. 1e, f). This exercise also verified that the peak CARS frequency is indeed at 1,600 cm^{-1}.

Due to its nonlinear optical origin, the CARS signal was generated only at the focal spot which is usually ~300–400 nm. As a result, the signal intensity was only dependent on the local molecular density, or concentration of molecular oscillators within the focal spot, not the sample thickness along the optical path. The CARS signals measured in this study, therefore, could be considered relatively quantitative. In addition, plant cell wall materials had only small absorption at the wavelengths of the two laser beams used for CARS (1,064 and 910 nm) which minimizes photo damage. In our study, there was no significant photo damage observed, and indeed, the CARS signal was consistent after 10 min of sample exposure to the lasers.

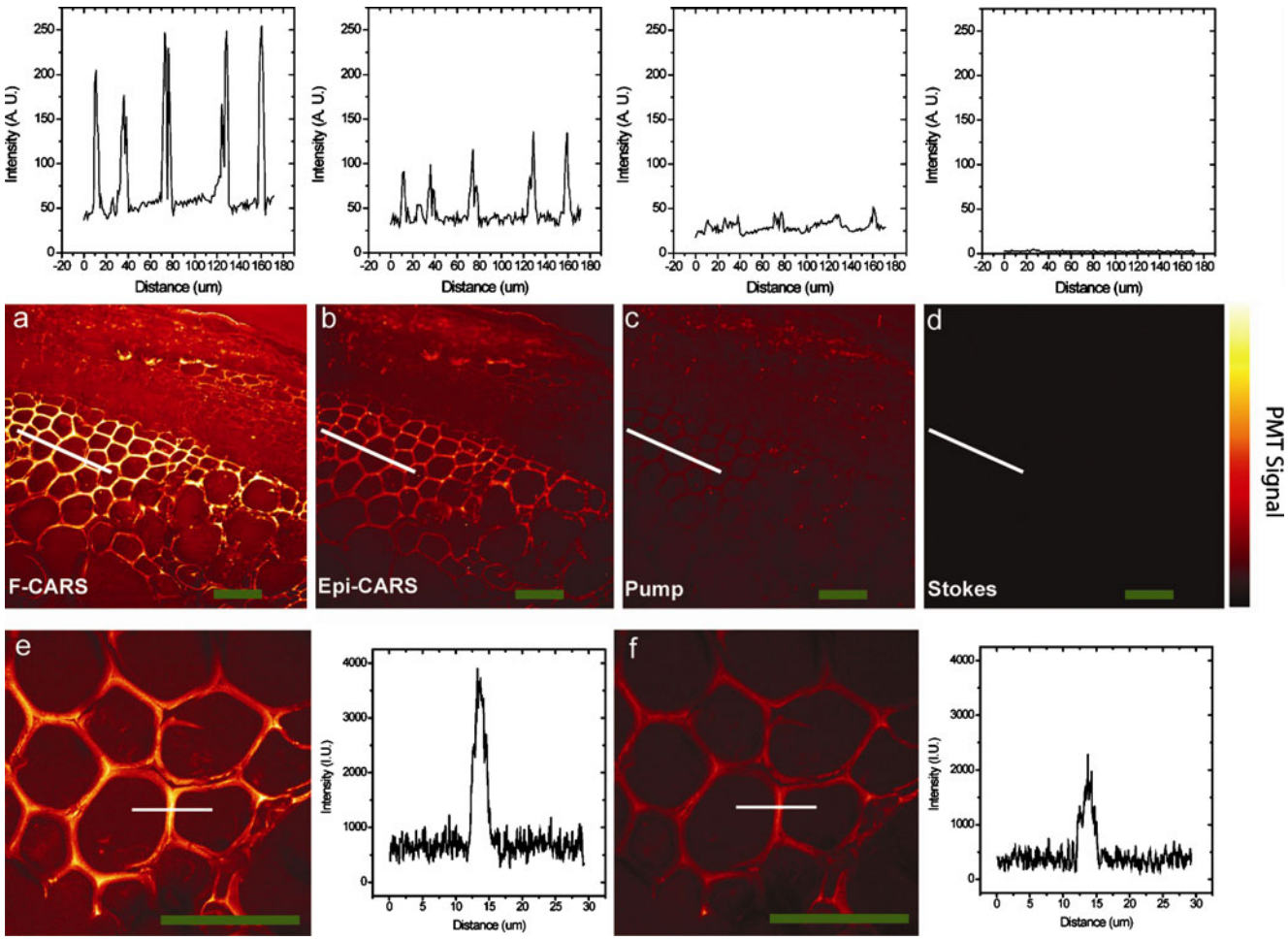

Fig. 1 **a**–**d** The specificity of the CARS signal compared to the fluorescence background was proven by imaging wild-type alfalfa cell walls. F-CARS (**a**) and Epi-CARS (**b**) are collected images obtained by exciting the sample with both pump and Stokes beams. **c** Multi-photon fluorescence (*MPF*) image obtained by exciting the sample with only the pump beam at 910 nm. **d** MPF image obtained by exciting the sample with only the Stokes beam at 1,064 nm. **e**, **f** Using wild-type alfalfa cell walls, the on-resonance CARS signal of lignin (tuning pump beam at 910 nm) (**e**) is compared with off-resonance background (tuning pump beam at 914 nm), both via Epi CARS (**f**). Scans across the cells as indicated by the *white lines* are shown above (**a**–**d**) or to the right of (**e**, **f**) the corresponding figures. *Scale bar* 50 μm

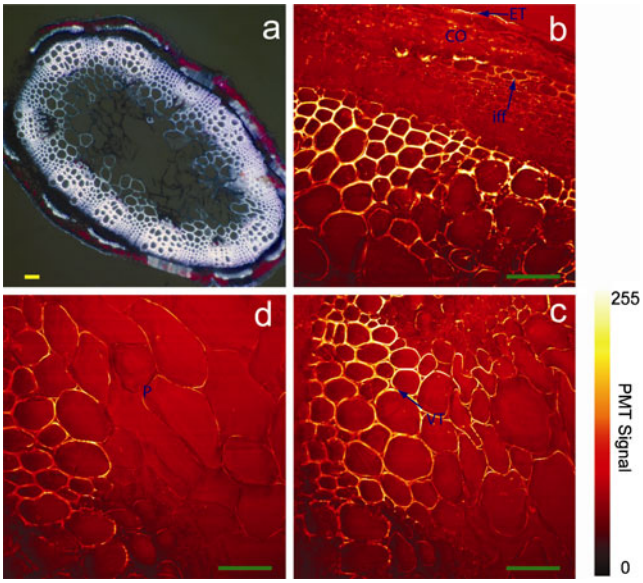

Fig. 2 **a** Auto-fluorescence image of the stem of WT alfalfa. **b**–**d**. F-CARS images of different areas of wild-type alfalfa stem (**b** epidermal tissue, cortex, and inter-fascicular fibers; **c** mainly vascular tissue; **d** mainly pith). The CARS signal is chemically selective, and the intensities of CARS in different tissues show notably different patterns from the autofluorescence. The highest CARS signal appears in lignified tissues. *Scale bar* 50 μm. Because the CARS objective has high numerical aperture and limited field of view, it is not possible to capture a whole stem image. The autofluorescence image was captured using a different apparatus which has a much lower magnification and can visualize the entire sample in one field of view. *CO* cortex, *ET* epidermal tissue, *iff* inter-fascicular fibers, *P* pith, *VT* vascular tissue

CARS images were taken at different areas across the stem, from epidermal tissue to the pith (Fig. 2). The CARS signal was primarily detected from lignified walls, such as the outer wall of the epidermis, vascular tissues (thick-walled elements), and fibers (vascular and inter-fascicular sclerenchyma). In general, the CARS intensity was found to be reduced relatively at the tissue level in the order fiber (highest) > xylem > epidermis > phloem > parenchyma and at the cellular level in the order cell corner (CC, highest) > compound middle lamella (CML, including middle lamellae and primary cell walls from adjacent cells) > secondary wall (SW). The CARS signal appeared homogenously distributed in the SW areas (mostly in the S2 layer) on both sides of the CML, which appeared as two flat shoulder peaks. In the pore areas, the pit membranes appeared to contain less lignin than the CML (Figs. 3 and 4). These observations provide direct visualization to support the previous argument from a study of *Pinus radiata* which proposed that lignification is initiated in the central zone of the CC-CML areas [16]. Compared to the WT control, the lignin-downregulated lines exhibited similar patterns of lignin distribution in the tissues studied.

The signal intensity distribution in the CC, CML, and SW areas of the inter-fascicular fiber cells was further analyzed using line scans across the cell wall. Figure 4 shows the line profiles of representative fiber cell walls. In the downregulated lines (HCT and C3H), the signal intensity distribution followed the same trend as that of the WT control without significant change in the wall thickness of the lignified cell wall types. Interestingly, the lignin CARS signal in the downregulated lines was not reduced equally in different areas of the cell walls. In the WT plant sample, the intercellular spaces at adjacent cells were mostly filled with lignified materials, whereas the triangular shape of the intercellular space was clearly visible in the downregulated lines. It was found that in the CC area, the estimated CARS signal intensity was reduced significantly more than that in the SW of both down-regulated lines. For example, compared to WT plants, both HCT and C3H lines shown more reduction of the CARS signal in the CC area than in the CML and SW areas. A slightly greater reduction in CARS signal intensity was observed in the CML and SW areas in the C3H line than in the HCT line.

Cell walls from HCT and C3H downregulated alfalfa lines have been shown to exhibit accessibility to acids and particularly to enzymatic hydrolysis [11]. However, down-regulation of lignin often affects plant performance and decreases biomass yields. The mechanisms underlying the relationship between lignin content and the hydrolysis process remain unknown. During biomass conversion, the transport of chemical/enzymatic catalysts within plant tissues is believed to be the critical initial step that affects

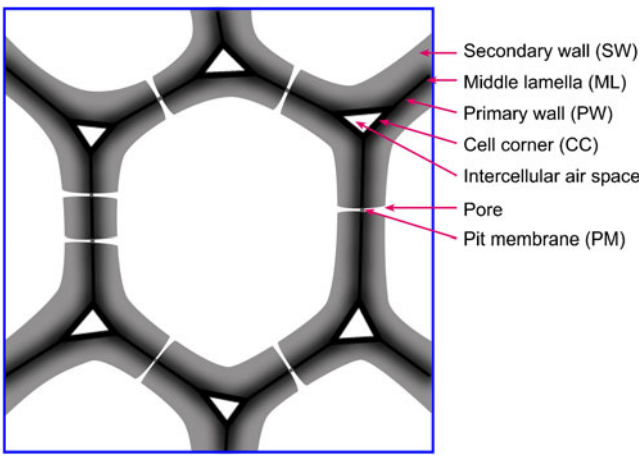

Fig. 3 Model structure of a cross-section of an inter-fascicular fiber cell showing lignin distribution in cell walls. The *grayscale* represents approximate lignin content based on the CARS signal intensities (Table 1). In this type of cell wall, lignin content decreases in the order CC (highest) > ML > PW > SW. The intercellular air space and pore structures of the cell walls are believed to permit transport of hydrolytic agents to their site of action during cell wall processing

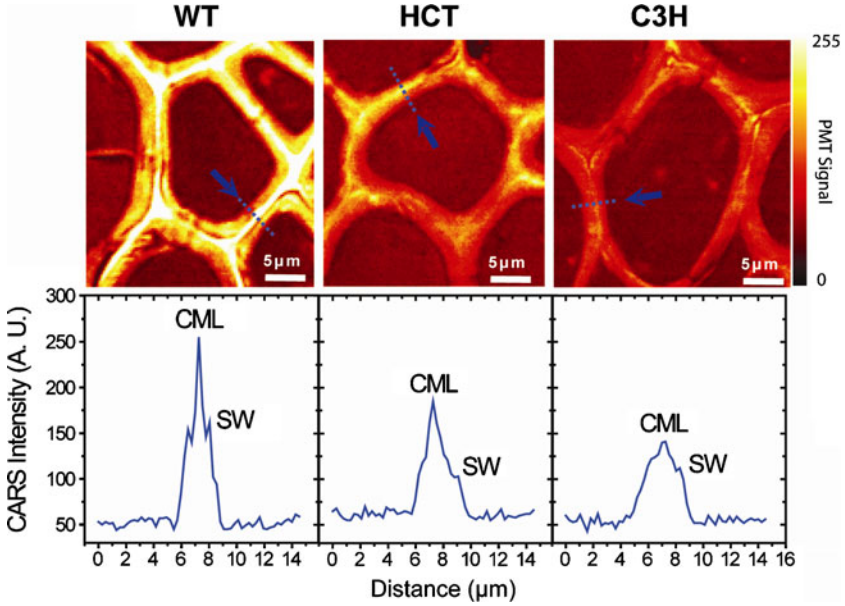

Fig. 4 *Top* CARS micrographs of lignin distribution in cross-sections of wild-type (*WT*) and lignin-downregulated alfalfa lines (HCT and C3H). *Bottom* Corresponding line profiles of CARS intensities show different lignin contents across the cell wall layers, in the direction shown by the *blue arrows*. The reduction of the CARS signal occurs specifically in CC and CML areas. *CML* compound middle lamella (middle lamella + primary walls), *SW* secondary wall. The CARS images were taken in 130×130 micron scans and cropped to show the representative cells

the efficiency of hydrolysis. It was reported that liquid transport in corn stover primarily follows the pathways established in the intercellular space (cell corners) and fissures formed during natural senescence and material handling [17]. One hypothesis could be that catalysts (chemicals and enzymes) initiate their action at the intercellular space, such as in the CC area. Hydrolysis would then have to follow a path from middle lamella to the primary cell wall and finally to the secondary cell wall. Therefore, it is reasonable to believe that reduction of lignin content in the CC area could potentially enhance the accessibility of catalysts, thus improving the hydrolysis rate at these critical areas. In this regard, CARS imaging can provide a direct visualization approach for biomass evaluation.

Conclusions

To the best of our knowledge, the current study is the first to demonstrate high spatial resolution chemical imaging of lignin in native plant cell walls that does not need any type of pretreatment in order to remove fluorescent pigment. In this methodology, the samples are freshly cut and imaged in water without any further preparation process to deal with fluorescence background issues, which ensures minimum damage to the native structure of the cell walls. CARS provides high chemical selectivity as well as high sensitivity, which allows for acquisition times in seconds per frame. CARS, therefore, is a promising tool to follow the progression of chemical pretreatment and enzymatic hydrolysis during the biomass conversion process. Multiple

Table 1 Average Epi-CARS intensity collected from cell corner (*CC*), compound middle lamella (*CML*), and secondary cell wall (*SW*) of interfascicular fiber cells (each including ten measurements on different spots), as illustrated in Fig. 4

Alfalfa samples	Overall signal of single cell wall[a]	Signal from different cell wall areas[b]		
		CC	CML	SW
WT	42±10	132	52	32
HCT	18±6	33	30	16
C3H	12±3	30	19	10

Epi-CARS images were obtained by setting Raman shift at 1,600 cm^{-1} to probe the lignin C=C symmetric stretch vibration

[a] Average signal per pixel measured from the overall cell wall region, including the cell corner, middle lamella, and secondary cell wall

[b] Average signal per pixel measured separately from the cell corner, middle lamella, and secondary cell wall

chemical compounds have been monitored during pretreatment by Fourier transform infrared spectroscopy [18]. However, due to its relatively slow data acquisition speed, imaging large areas at high resolution was not possible. Therefore, the chemical content at multiple sites in the tissue cannot be monitored simultaneously to compare different structures. Because of the strong signal in CARS, which allows fast imaging, the trends in the distribution of one compound can be monitored across different cell wall locations almost simultaneously (within a few seconds). Because CARS does not require extensive sample preparation, it could also be integrated into new high-throughput technologies designed to evaluate lignocellulosic materials.

As we have demonstrated here, CARS microscopy offers high resolution and chemical specificity for high concentration species such as lignin in plant cell walls. However, CARS imaging suffers from a non-resonant electronic background [4] that can limit the sensitivity for low concentration species by providing a non-specific background signal. Many methods exist to deal with this background and improve the sensitivity and quantitation of coherent Raman imaging, including stimulated Raman scattering [19], which could also be applied to biomass for detecting the presence of other components of the plant which exist at lower levels.

Acknowledgments The authors thank Gary R. Holtom from Harvard University for his help and valuable discussion on CARS setup. The authors gratefully acknowledge the US Department of Energy, the Office of Science, Office of Biological and Environmental Research through the BioEnergy Science Center (BESC), a DOE Bioenergy Research Center, for the work on CARS imaging and analysis, and grant DE-FG02-07ER64500 for support to develop the CARS microscope.

References

1. Perlack RD, Wright LL, Turhollow AF, Graham RL, Stokes BJ, Erbach DC (2005) Biomass as feedstock for a bioenergy and bioproducts industry: the technical feasibility of a billion-ton annual supply. DOE/GO-102005-2135, ORNL/TM-2005/66
2. Foust TD, Ibsen KN, Dayton DC, Hess JR, Kenny KE (2008) The biorefinery. In: Himmel ME (ed) Biomass recalcitrance: deconstructing the plant cell wall for bioenergy. Blackwell, Oxford, pp 7–37
3. Ding S-Y, Xu Q, Crowley M, Zeng Y, Nimlos M, Lamed R et al (2008) A biophysical perspective on the cellulosome: new opportunities for biomass conversion. Curr Opin Biotechnol 19(3):218–227
4. Cheng J-X, Xie XS (2004) Coherent anti-Stokes Raman scattering microscopy: instrumentation, theory, and applications. J Phys Chem B 108(3):827–840
5. Cheng J-X, Volkmer A, Book LD, Xie XS (2001) An Epi-detected coherent anti-Stokes Raman scattering (E-CARS) microscope with high spectral resolution and high sensitivity. J Phys Chem B 105:1277–1280
6. Ding S-Y, Himmel ME (2006) The maize primary cell wall microfibril: a new model derived from direct visualization. J Agr Food Chem 54(3):597–606
7. Chabannes M, Barakate A, Lapierre C, Marita JM, Ralph J, Pean M et al (2001) Strong decrease in lignin content without significant alteration of plant development is induced by simultaneous down-regulation of cinnamoyl CoA reductase (CCR) and cinnamyl alcohol dehydrogenase (CAD) in tobacco plants. Plant J 28(3):257–270
8. Jones L, Ennos AR, Turner SR (2001) Cloning and characterization of irregular xylem4 (irx4): a severely lignin-deficient mutant of *Arabidopsis*. Plant J 26(2):205–216
9. Himmel ME, Ding S-Y, Johnson DK, Adney WS, Nimlos MR, Brady JW et al (2007) Biomass recalcitrance: engineering plants and enzymes for biofuels production. Science 315(5813):804–807
10. Li X, Weng J-K, Chapple C (2008) Improvement of biomass through lignin modification. Plant J 54(4):569–581
11. Chen F, Dixon RA (2007) Lignin modification improves fermentable sugar yields for biofuel production. Nat Biotechnol 25(7):759–761
12. Chen F, Srinivasa Reddy MS, Temple S, Jackson L, Shadle G, Dixon RA (2006) Multi-site genetic modulation of monolignol biosynthesis suggests new routes for formation of syringyl lignin and wall-bound ferulic acid in alfalfa (*Medicago sativa* L.). Plant J 48(1):113–124
13. Boudet AM, Lapierre C, Grima-Pettenati J (1995) Tansley review No-80—biochemistry and molecular-biology of lignification. New Phytol 129(2):203–236
14. Agarwal UP (2006) Raman imaging to investigate ultrastructure and composition of plant cell walls: distribution of lignin and cellulose in black spruce wood (*Picea mariana*). Planta 224 (5):1141–1153
15. Gierlinger N, Schwanninger M (2006) Chemical imaging of poplar wood cell walls by confocal Raman microscopy. Plant Physiol 140(4):1246–1254
16. Donaldson LA (1994) Mechanical constraints on lignin deposition during lignification. Wood Sci Technol 28(2):111–118
17. Viamajala S, Selig M, Vinant T, Tucker M, Himmel M, McMillan J et al (2006) Catalyst transport in corn stover internodes. Appl Biochem Biotechnol 130(1):509–527
18. Gierlinger N, Goswami L, Schmidt M, Burgert I, Coutand C, Rogge T et al (2008) In situ FT-IR microscopic study on enzymatic treatment of poplar wood cross-sections. Biomacromolecules 9(8):2194–2201
19. Freudiger CW, Min WS, Brian G, Lu SH, Gary R, He C et al (2008) Label-free biomedical imaging with high sensitivity by stimulated Raman scattering microscopy. Science 322(5909): 1857–1861